Cooling Potential of Solar-Ice Systems in Multi-Family Buildings

Mattia Battaglia, Jeremias Schmidli, Maike Schubert and Daniel Carbonell

Institut für Solartechnik (SPF), Ostschweizer Fachhochschule (OST),
CH-8640 Rapperswil, Switzerland

Abstract

Solar-ice systems are an emerging technology to provide renewable heat. Storing the ice that is generated during the heating season until summer can help to cover the increasing cooling demand in residential buildings. The potential of this approach is analyzed based on dynamic yearly system simulations in TRNSYS. Two different control strategies are discussed for three different locations in Switzerland. The results demonstrate that a passive cooling approach can provide cooling that is sufficient for a well insulated multi-family building in Zurich with little additional costs. To increase the cooling potential of the system, the heat pump operation for domestic hot water preparation can be used during the summer months.

Keywords: ice storage, solar heating and cooling, system simulation

Nomenclature

A_{coll}	collector area	V_{ice}	ice storage volume
Q_{sc}	space cooling energy	$Q^{heat,pri}_{ice-storage}$	heat from primary loop to ice storage
$Q^{gains}_{ice-storage}$	heat gains ice storage wall	$Q^{cool,pri}_{ice-storage}$	cold from primary loop to ice storage
$Q^{losses}_{ice-storage}$	heat losses ice storage wall	Q^{acum}_{ice}	ice storage total accumulated cooling energy
Q_{dhw}	domestic hot water demand	Q^{loss}_{circ}	circulation losses
Q_{sh}	space heating demand	Q_{sc}	space cooling demand
$Q_{ice-storage,walls}$	total energy transfer walls	Q_{col}	solar collector gains
$El_{Hp,comp}$	el. consumption heat pump	$El^{Aux}_{Tes,sh}$	el. consumption auxiliary heater sh
$El^{Aux}_{Tes,dhw}$	el. consumption auxiliary heater dhw	SPF	system performance factor

doi:10.18086/eurosun.2020.01.13 Available at http://proceedings.ises.org

1. Introduction

Ice storages are a well proven technology for cooling applications where their main role consists in peak shaving of cooling loads at noon or in providing high cooling power for industrial processes. On the other hand, an ice storage can also be used for solar heating applications which is a promising way to increase the share of renewable energy in buildings. It has been demonstrated that the system can reach a yearly average performance that is comparable to ground source systems by making use of the latent heat that is released during icing as a source for the heat pump (Abrahamsson et al., 1981, Carbonell et al., 2016b). In future climate scenarios, increased cooling demand during summer will lead to increased stress in energy supply systems (Jakubcionis and Carlsson, 2017). Therefore, new approaches for energy efficient cooling are needed. In this study, it is analyzed if the ice produced in the ice storage of a solar-ice system during the heating season can be stored during spring and used for cooling during summer with minimal additional energy consumption.

2. Solar ice-system system concept

The solar-ice system investigated has been subject of several experimental and modelling studies (Carbonell et al., 2016a, 2014). This study builds on a recent publication in which different hydraulic layouts of the system were tested for their performance to meet the demand of a multi-family building (Carbonell et al., 2019). To provide solar-ice systems the cooling functionality, the ice produced in the heating season is stored for later use in the cooling season. Thus, the ice storage can not serve as a heat sink for the evaporator during this period. Therefore, the system layout needs to provide a connection of the solar collector to the heat pump. For the simulations described in this report, the archetype that is shown in Figure 1 was used. In this variant of a solar-ice system, the heat of the solar collector can be delivered to three different heat sinks: to the thermal energy storages, to the evaporator of the heat pump or to the ice storage.

The physical layout that was simulated is shown in Figure 2. The only renewable heat source of the system is the solar collector field, that with first priority delivers heat to the heat pump evaporator in winter periods. If the outlet temperature of the solar collector is high enough, the solar thermal energy is used to charge the domestic hot water storage and with second priority the space heating storage. If the source temperature provided by the solar collector drops below the minimal evaporator input temperature, the collector operation is stopped and the heat pump runs completely using the ice storage. The domestic hot water is delivered by an external heat exchanger unit. On the demand side of the external domestic hot water heat exchanger, fast availability of hot water during tapping is guaranteed by a circulation loop. In time steps with no tapping, a second double port is used in the domestic hot water storage tank to account for the higher return temperatures of the circulation loop.

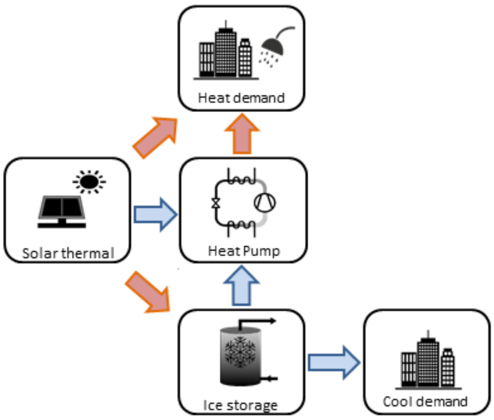

Fig. 1: Simplified solar-ice system concept.

In order to use the solar-ice system for cooling during summer, two different control strategies have been analyzed. They both extend a base solar-ice control that was described in detail in Philippen et al. (2015) for the particular case of thermal-deicing and in Carbonell et al. (2017a) without the deicing functionality. Since cooling exhibits high peak power during summer, large heat exchanger areas are necessary in the system. Therefore, for this double purpose system, a system without deicing is considered in which the heat exchangers cover the whole storage volume. During normal heating operation the control has the following three priorities

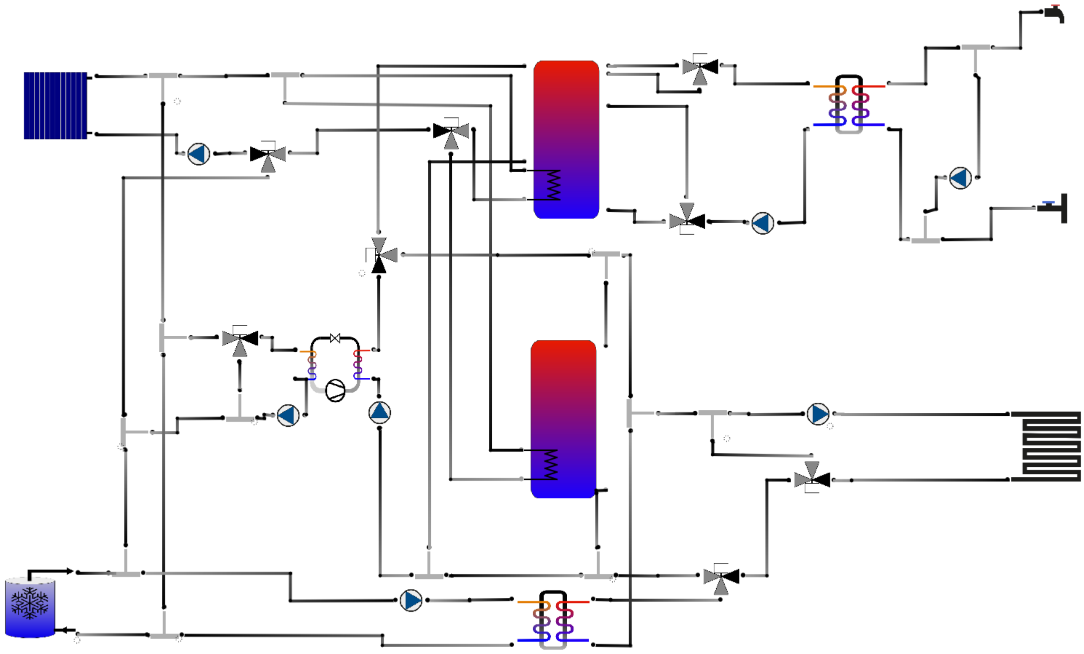

Fig. 2: Hydraulic scheme of the simulation.

1. Use the solar heat for direct charging of the domestic hot water storage.
2. Use the solar heat for direct charging of the space heating storage (only during heating season).
3. Switching on the heat pump when needed to provide the heat demand with the solar collectors as the main heat source.
4. Operate the heat pump with the ice storage as the main heat source in case of too low source temperatures of the solar collectors.
5. Use the low-grade solar heat to load/regenerate the ice storage.

The cooling was added to the control by avoiding active regeneration of the ice storage below an ice fraction of 50 % from March to September to preserve the ice in the latent storage. Some ice melting from the maximum ice fraction of 80 % to 50 % was included to still enable heat extraction in case of high heating demand during March and April.

The first cooling strategy is the **passive cooling** mode. In this approach, no additional changes besides the stopping of the ice storage charging in spring are present. The goal of this strategy is to cover as much demand as possible by simply storing the ice in the ice storage from the heating period to the cooling period. This approach will have only little influence on the SPF of the heating system but the total amount of cooling capacity will be strictly limited to the ice storage volume and the heat gains from the ground during spring.

Since for many applications, the passive cooling approach will not be able to cover the cooling demand, the cooling by a heat pump in DHW mode was added as a second control strategy. In this mode, in addition to the changes described for the first mode, the direct charging of the domestic hot water storage tank by solar collectors is completely suppressed during the summer months. In fact, solar collectors are not used at all during summer months, not even as a heat source for the heat pump to provide the DHW demands. This forces the heat pump to extract heat from the ice storage during the preparation of domestic hot water which will add more cooling capacity to the system. However, this will result in a decreased overall system efficiency SPF_{SHP+} since the heat pump will run in time periods where solar collectors could cover the DHW demand more energetically efficient.

2.1. *Performance indicators*

The main performance indicator for the systems is the System Performance Factor calculated as described in Malenkovic et al. (2012):

$$SPF_{SHP+} = \frac{Q_{DHW} + Q_{SH}}{P_{el,T}} = \frac{Q_D}{P_{el,T}} \tag{1}$$

Q is the yearly heat demand and $P_{el,T}$ the yearly electricity consumption of the heating system. The subscripts SHP, DHW, SH and D stand for solar and heat pump, domestic hot water, space heating, and total demand respectively.

The yearly electricity consumption is calculated as:

$$P_{el,T} = P_{el,pu} + P_{el,hp} + P_{el,cu} + P_{el,back-up} + P_{el,pen} \tag{2}$$

where the subscripts pu, hp, cu, aux and pen refer to circulation pumps, heat pump, control unit, back-up and penalties respectively. The symbol "+" in the SHP+ from Eq. 1 refers to the consideration of the heat distribution circulating pump in the electricity consumption. Therefore, the system performance indicator used in this work includes all circulation pumps of the system and also all thermal losses/gains from storages and piping. Penalties for not providing the heating demand at the desired comfort temperature are calculated according to Haller et al. (2012). $P_{el,back-up}$ is the energy used from the direct electric back-up system. This back-up is implemented with two electrical rods for DHW and SH in the storage. The back-up is switched on when the temperature of the brine at the inlet of the evaporator drops below -8 °C. This is the case when the ice storage is at its maximum allowed ice fraction and the energy gained in the collector field is not sufficient (night or foggy times with low ambient temperatures).

3. Simulation model

The simulations were done in TRNSYS 17 (Klein et al., 2010) using the open source python framework pytrnsys (Carbonell et al., 2020). The pytrnsys framework allows the fast and efficient simulation and processing of parametric runs by splitting the TRNSYS dck file into component specific ddck files. The simulation timestep was set to 2 minutes in all simulations. In total 14 months starting from July were simulated to ensure correct initialization of the ice storage. The results were taken from the last 12 months of the simulation starting in September.

3.1. *Weather data and building model*

The building simulated is the reference multi-family building MFB30 (Iturralde et al., 2019). The building represents a typical swiss multi-family building with 6 flats and high insulation standard. For the study of the cooling potential three locations in Switzerland with different characteristics were included. Zurich represents the climatic conditions of the densely populated Swiss midlands with medium heating demand and low cooling demand. The city of Geneva is included as an example of slightly warmer climatic conditions with medium heating demand and medium cooling demand. The location of Locarno in the Swiss south has reduced heating demand and increased cooling demand compared to other Swiss cities while still being in a heating dominant region. The heating set point temperature was at 21 °C and the cooling set point temperature at 24 °C. The

Tab. 1: Heating and cooling demand of the MFB30 building in the three cities.

Month	Zurich (SMA)		Geneva (GVE)		Locarno (OTL)		DHW
	Heat (kWh)	Cold (kWh)	Heat (kWh)	Cold (kWh)	Heat (kWh)	Cold (kWh)	(kWh)
Jan	6741	0	5858	0	5328	0	1581
Feb	5281	0	4554	0	3104	0	1347
Mar	3521	0	2097	0	1221	0	1406
Apr	4845	0	3862	0	2767	0	1460
May	1919	0	1287	0	550	60	1535
Jun	65	604	0	1092	0	2137	1460
Jul	0	1198	0	2663	0	2985	1351
Aug	0	712	0	1879	0	3582	1577
Sept	1074	0	507	0	0	0	1363
Oct	1906	0	741	0	251	0	1558
Nov	4458	0	3943	0	2995	0	1398
Dec	6373	0	5649	0	5028	0	1525
Total	36187	2514	28501	5634	21247	8764	17564

summary of the resulting demands of the three different locations can be found in Table 1.

3.2. Ice Storage Model

The ice storage model used is described in detail in Carbonell et al. (2018). For the simulations a capillary mat model was used. The distance between the capillary mats was set to 10 cm. The distances between the capillary pipes in the mat was assumed to be 3 cm according to products available on the market. The total ice storage volume was set relative to the yearly heating and domestic hot water demand expressed in MWh. Values in the range of $0.5\,m^3/MWh$ to $1\,m^3/MWh$ were investigated that were found to lead to systems that are economically competitive compared to ground source heat pump systems(Carbonell et al., 2017b). The ice storage was assumed to have a quadratic layout and a height of 2.5 m.

Furthermore, it was assumed that the ice storage is buried in the ground next to the building. The ice storage is insulated with a foam of heat conductivity $0.041\,W/(mK)$ and thickness 5 cm resulting in a U-value of $0.82\,W/(m^2K)$. The ground model and the used parametrization is described in detail in Carbonell et al. (2016b).

4. Results

As a base case, a system dimensioned to economically and energetically compete to ground source systems has been simulated (Carbonell et al., 2017b). The ice storage volume was set to $0.5\,m^3/MWh$ which in the location of Zurich resulted in a total volume of $27\,m^3$. The collector area was set to $1.75\,m^2/MWh$ which led to a size of 93 m^2. The overall heat balance of the passive cooling system in the location of Zurich is shown in Figure 3. The heat sources of the system are the collector gains Q_{col}, the electricity consumption of the heat pump $El_{Hp,comp}$ as well as the auxiliary heaters in the space heating tank $El^{Aux}_{Tes,sh}$ and the domestic hot water tank $El^{Aux}_{Tes,dhw}$. The heat sinks of the system are the domestic hot water demand Q_{dhw}, the space heating demand Q_{sh} and the circulation losses Q^{loss}_{circ}. Depending on the average state of the ice storage in a month, the accumulated heat $Q^{acum,sens+lat}_{ice-storage}$ and the heat transfer through the ice storage wall $Q_{ice-storage,walls}$ can have positive or negative monthly values. In Fig. 3 the pipe and the losses of the thermal storage have been omitted as they have only a minor effect on the yearly scale. The results show, that with the chosen system size the ice storage starts to be fully iced in January and the electric backup has to provide some of the heat during the winter months. This is a result of the sizing concept that aims to reduce the cost of the solar ice system and to make it economically more attractive while reaching SPF_{SHP+} in the range of ground source heat pumps.

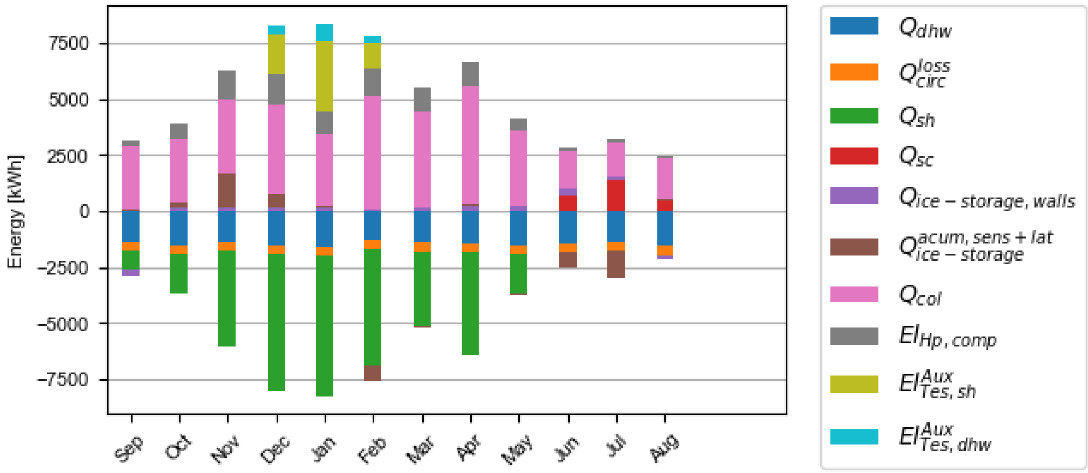

Fig. 3: Heat balance of the passive cooling system in Zurich.

4.1. Passive cooling

In order to analyze in detail the cooling potential of the passive control approach, the corresponding energy balance of the ice storage is shown in Figure 4. The balance involves the cold $Q_{sc}^{extracted}$ delivered by the ice storage to the space cooling system, the heat gains and losses through the ice storage wall $Q_{walls}^{gains/losses}$, the heat and cold delivered to the ice storage by the solar collector and the heat pump $Q_{col}^{delivered}/Q_{hp}^{extracted}$ as well as the cooling energy accumulated in the ice storage $Q^{acum, sens+lat}$. Figure 4 shows the monthly cumulative values starting from September. The total amount of heat extracted from the ice storage between September and January adds up to 2526 kWh. While this exceeds the total cooling demand of 2514 kWh in Zurich, not all energy is kept during spring. In the months between February and May 674 kWh of cooling energy in the ice storage are lost due to natural melting by heat gains from the ground. In addition, a warm period is present in late February in the weather data that was used for Zurich. Since the used cooling control stops normal operation to prevent melting not before the beginning of March this leads to some active regeneration of the ice storage. Part of the losses in stored ice capacity are compensated by some additional heat that is extracted during spring due to the heat pump operation, mostly for space heating.

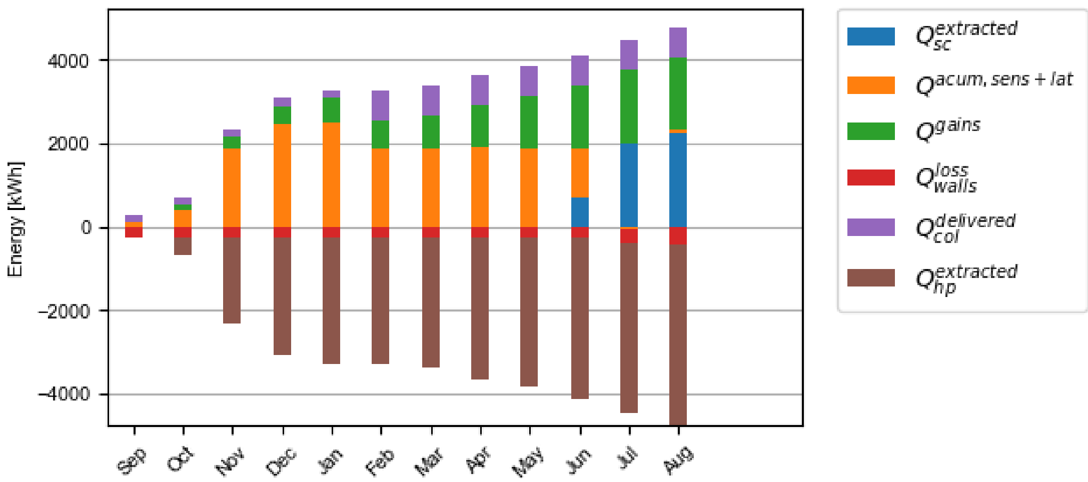

Fig. 4: Heat balance on the ice-storage of the passive cooling system in Zurich.

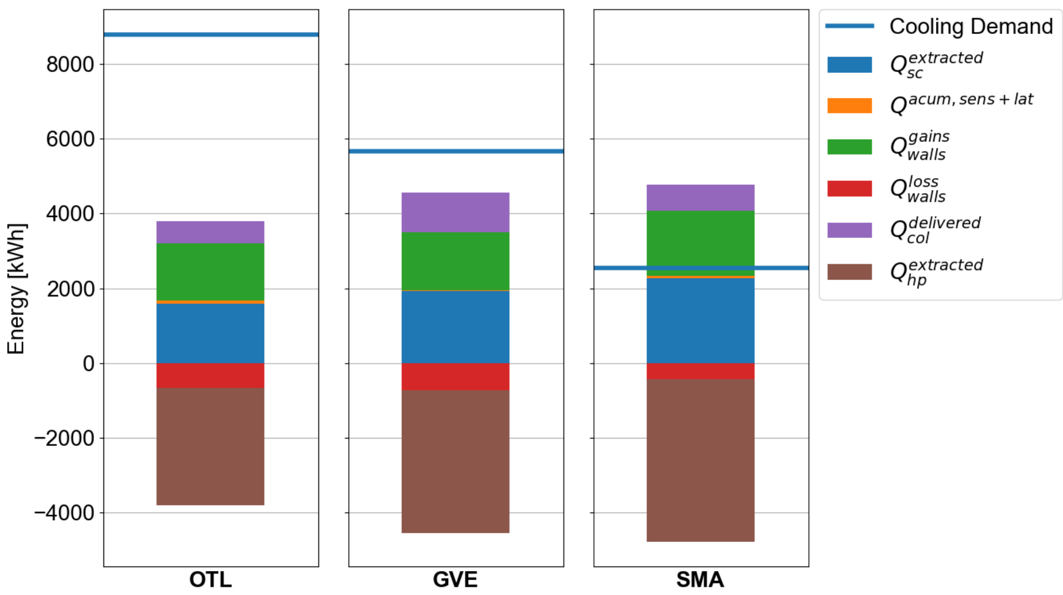

Fig. 5: Final cumulative heat balance after one year of the passive cooling strategy in Zurich (SMA, V_{ice}=26.6 m^3, A_{col}=93.1 m^2), **Geneva (GVE,** V_{ice}=22.8 m^3), A_{col}=79.6 m^2) **and Locarno (OTL,** V_{ice}=19.1 m^3, A_{col}=67.0 m^2).

Tab. 2: Summary of provided cooling energy and corresponding SPFs for the simulated system variants.

Strategy	V_{ice}	A_{col}	Zurich (SMA)		Geneva (GVE)		Locarno (OTL)	
			Cold	SPF_{SHP+}	Cold	SPF_{SHP+}	Cold	SPF_{SHP+}
	m^3/MWh	m^2/MWh	kWh	-	kWh	-	kWh	-
No Cooling	0.5	1.75	-	3.3	-	4.3	-	5.6
Passive Cooling	0.5	1.75	2485	3.2	2133	4.1	1797	5.4
Passive Cooling	1.0	1.5	2730	3.3	3633	4.4	3267	5.2
Cooling-By-Hp	0.5	1.75	2916	3.0	4635	3.8	5141	4.8

In Figure 5, the cumulated monthly balance results for one completed year are shown for different locations. The overall results shows that the passive cooling approach is approximately able to provide the defined cooling demand in Zurich but not the higher cooling demands in Locarno (OTL) and Geneva (GVE). The total cooling energy delivered by the system in Locarno and Geneva is even lower than that of Zurich due to the lower ice storage volume used. Notice that ice storage volume is sized with respect to the heating demand and this is lower in Geneva and Locarno compared to Zurich. The effect of the passive cooling strategy on the yearly SPF of the system is given in Table 2. The results confirm that the passive cooling does not affect the SPF significantly, showing deviations from the system without cooling of below 5 %.

Since the cooling potential in the passive cooling approach is limited by the ice volume in the end of the heating season, a larger ice storage volume of 1 m^3/MWh in combination with a reduced collector area of 1.5 m^2/MWh has been investigated. The results of the simulations are shown in Figure 6. It can be seen that increasing the storage size while reducing the collector area can significantly increase the cooling potential of the system. However, in the case of Locarno, the decreased collector area had a negative influence on the SPF_{SHP+}. Notice that the reduction of the collector field is proposed to keep the installation cost similar when increasing the ice storage with the added benefit of being able to provide more cooling demand for *free*.

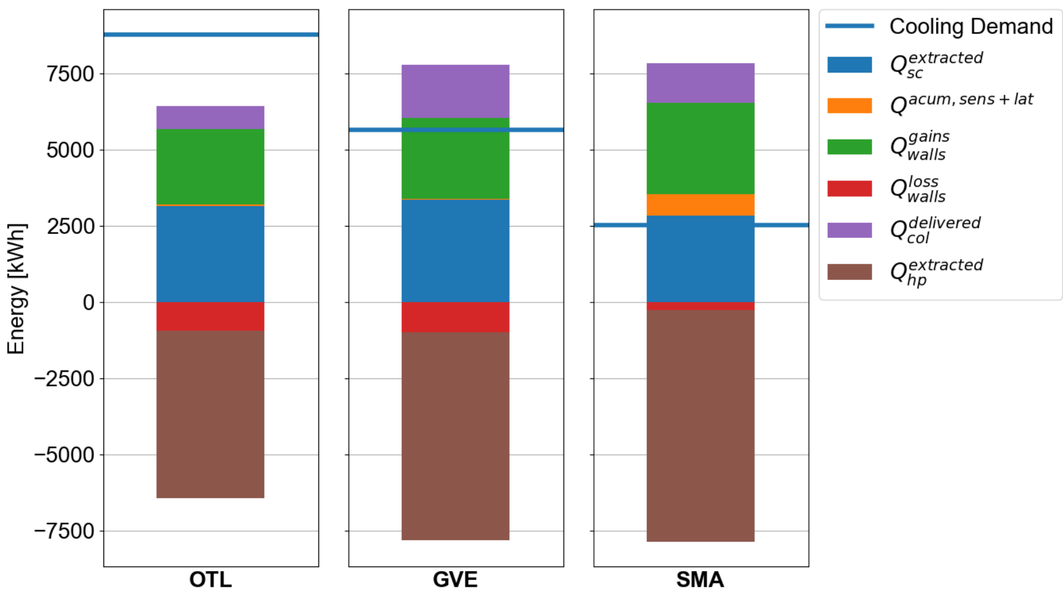

Fig. 6: Final cumulative heat balance after one year of the passive cooling strategy using an ice storage volume of $1.0\,\mathrm{m^3/MWh}$ **and a collector area of** $1.5\,\mathrm{m^2/MWh}$ **in Zurich** $(\mathrm{SMA}, V_{ice} = 53.2\,\mathrm{m^3}, A_{col} = 79.8\,\mathrm{m^2})$**, Geneva** $(\mathrm{GVE}, V_{ice} = 45.5\,\mathrm{m^3}, A_{col} = 68.3\,\mathrm{m^2})$ **and Locarno** $(\mathrm{OTL}, V_{ice} = 38.2\,\mathrm{m^3}, A_{col} = 57.4\,\mathrm{m^2})$

4.2. Cooling by heat pump in domestic hot water mode

The comparison of the results for the three different locations with the cooling by the heat pump in domestic hot water strategy are shown in Figure 7. The simulations show that the cooling energy provided in Geneva and Locarno is increased by 2503 kWh and 3344 kWh respectively. These results correspond well to the total amount of domestic hot water demand during the cooling season of 5484 kWh which, in combination with the heat pump coefficient of performance map, sets an upper limit to the potential increase of available cooling energy compared to the passive cooling case.

The increased use of the heat pump for domestic hot water preparation reduces the overall system performance of the heating system as can be seen in Table 2. The decrease in SPF now exceeds 10 % in all locations as can be seen in Table 2.

5. Conclusions

The presented system simulations demonstrate the general potential of the solar-ice system for cooling application. Using an economically feasible dimensioning of the system, sufficient cooling can be provided for location with low demand like Zurich by simply stopping the active melting of the ice during spring. This approach has the advantage of not reducing the $\mathrm{SPF_{SHP+}}$ of the heating system significantly as well as affording minimal additional costs for implementation.

A passive cooling approach is not sufficient to cover the demand in locations with higher cooling demand such as Geneva or Locarno. If the ice storage volume is defined according to the heating demand, the lower ice capacity available from heating in a warmer climate does not help to deal with higher cooling demand during summer. Some optimization can be made by increasing the ice storage volume and enhancing the heat extraction of the heat pump during the heating season. However, this measures also lead to additional costs and it would have to be evaluated if such systems would be economically competitive.

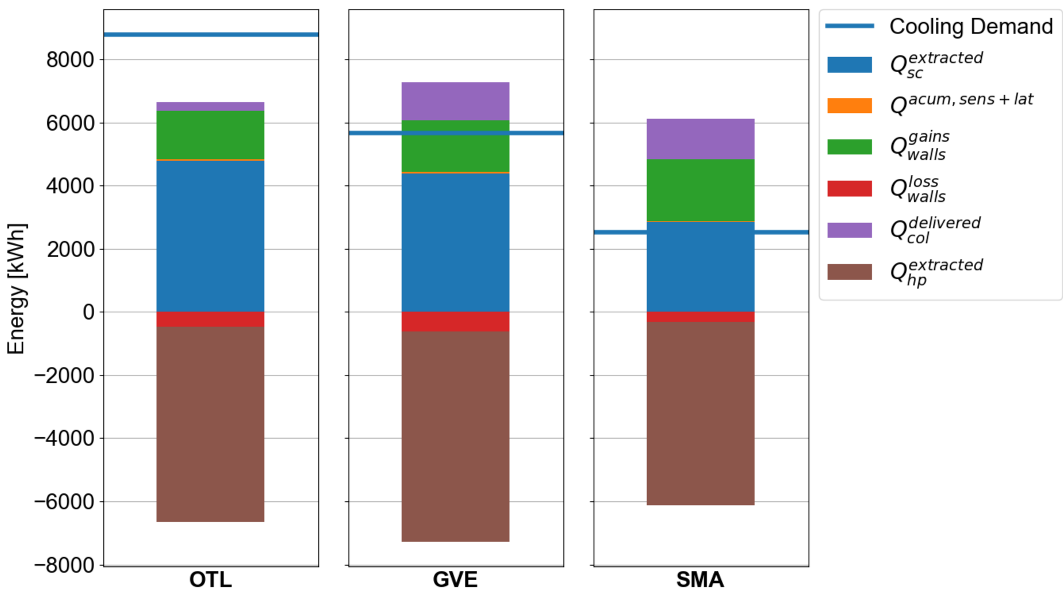

Fig. 7: Final cumulative heat balance after one year of the Cooling-By-Hp strategy using an ice storage volume of $0.5\,m^3/MWh$ **and a collector area of** $1.75\,m^2/MWh$ **in Zurich** (SMA, $V_{ice} = 26.6\,m^3, A_{col} = 93.1\,m^2$)**, Geneva** (GVE, $V_{ice} = 22.8\,m^3, A_{col} = 79.6\,m^2$) **and Locarno** (OTL, $V_{ice} = 19.1\ m^3, A_{col} = 67.0\ m^2$)

By using the cold of the heat pump evaporator during the summer months, the cooling potential of the system can be more than doubled. Since the heat pump replaces freely available heat from the solar collector, such an approach leads to a decreased SPF_{SHP+} of the system. Whether such an approach is economically beneficial will largely depend on the case-to-case basis and should be considered in future works.

Acknowledgments

The authors would like to thank the Swiss Federal Office of Energy (SFOE) for the financing support received under the project BigIce.

References

Abrahamsson, T., Jonson, S., Lagerkvist, K.O., 1981. Heat from solar energy and air with storage in water and ice, The Bramhult project in Boras: design, building, and performance evaluation of a Swedish solar energy and heat pump system for six detached houses. Swedish Council for Building Research in Stockholm, Sweden.

Carbonell, D., Battaglia, M., Daniel, D.P., Haller, M.Y., 2017a. Ice-Ex - Heat Exchanger Analyses for Ice Storages in Solar and Heat Pump Applications. Institut für Solartechnik SPF for Swiss Federal Office of Energy (SFOE), Research Programme Solar Heat and Heat Storage, CH-3003 Bern.

Carbonell, D., Battaglia, M., Philippen, D., Haller, M., 2018. Numerical and experimental evaluation of ice storages with ice on capillary mat heat exchangers for solar-ice systems. International Journal of Refrigeration 88, 383 – 401.

Carbonell, D., Battaglia, M., Schmidli, J., Schubert, M., Neugebauer, M., 2020. pytrnsys. `https://github.com/dcarbonellsanchez/pytrnsys`.

Carbonell, D., Granzotto, M., Battaglia, M., Philippen, D., Haller, M.Y., 2016a. Experimental investigations of heat exchangers in ice storages for combined solar and heat pump systems., in: 11^{th} ISES EuroSun Conference, International Solar Energy Society (ISES), Palma (Mallorca), Spain.

Carbonell, D., Philippen, D., Battaglia, M., Haller, M.Y., 2017b. Cost energetic analyses of ice storage heat exchangers in solar-ice systems, in: ISES Conference Proceedings. International Conference on Solar Heating and Cooling for Buildings and Industry (SHC 2017), Abu Dhabi, United Arab Emirates.

Carbonell, D., Philippen, D., Granzotto, M., Haller, M.Y., Frank, E., 2014. Simulation of combined solar thermal, heat pump, ice storage and waste water heat recovery systems. Design criteria and parametric studies., in: Proceedings of EuroSun, International Solar Energy Society (ISES), Aix les Bains, France.

Carbonell, D., Philippen, D., Haller, M.Y., 2016b. Modeling of an ice storage buried in the ground for solar heating applications. Validations with one year of monitored data from a pilot plant. Solar Energy 125, 398–414.

Carbonell, D., Schmidli, J., Philippen, D., Haller, M., 2019. Solar-ice systems for multi-family buildings: hydraulics and weather data analysis. E3S Web of Conferences 111, 01013.

Haller, M.Y., Dott, R., Ruschenburg, J., Ochs, F., Bony, J., 2012. The reference framework for system simulation of the IEA SHC Task44/HPP Annex 38: Part A : General simulation boundary conditions. Technical Report IEA-SHC Task44 Subtask C.

Iturralde, J., Alonso, L., Carrera, A., Salom, J., Battaglia, M., Carbonell, D., 2019. Energy demands for multi-family buildings in different climatic zones. Deliverable D1.1 of H2020 TRI-HP (www.tri-hp-eu). https://doi.org/10.5281/zenodo.3763249 .

Jakubcionis, M., Carlsson, J., 2017. Estimation of European Union residential sector space cooling potential. Energy Policy 101, 225–235.

Klein et al., 2010. TRNSYS 17: A Transient System Simulation Program, Solar Energy Laboratory. Technical Report. University of Wisconsin, Madison, USA, http://sel.me.wisc.edu/trnsys.

Malenkovic, I., Eicher, S., Bony, J., 2012. Definition of main system boundaries and performance figures for reporting on SHP systems. IEA-SHC Task44 Subtask B.

Philippen, D., Carbonell, D., Granzotto, M., Zenhäusern, D., Haller, M.Y., Brunold, S., 2015. High-Ice - System development for high solar thermal gains with ice storage and heat pump. Institut für Solartechnik SPF for Swiss Federal Office of Energy (SFOE), Research Programme Solar Heat and Heat Storage, CH-3003 Bern.